Contents lists available at ScienceDirect

Electrochemistry Communications

journal homepage: www.elsevier.com

Microwave-assisted sol-gel synthesis of an Au-TiO_2 photoanode for the advanced oxidation of paracetamol as model pharmaceutical pollutant

Rafael Hernández[a], Isidoro Olvera-Rodríguez[a], Carlos Guzmán[a], Alejandro Medel[b], Luis Escobar-Alarcón[c], Enric Brillas[d, 1], Ignasi Sirés[d, *, 1], Karen Esquivel[a, *]

[a] Posgrado de Ingeniería, Facultad de Ingeniería, Universidad Autónoma de Querétaro, Cerro de las Campanas, C.P. 76010 Santiago de Querétaro, Qro., Mexico
[b] Centro de Investigaciones y Desarrollo Tecnológico en Electroquímica, Parque Tecnológico Querétaro s/n, Sanfandila, Pedro Escobedo C.P. 76730, Qro., Mexico
[c] Departamento de Física, Instituto Nacional de Investigaciones Nucleares, Carretera México – Toluca s/n, La Marquesa Ocoyoacac, Mexico
[d] Laboratori d'Electroquímica dels Materials i del Medi Ambient, Departament de Química Física, Facultat de Química, Universitat de Barcelona, Martí i Franquès 1-11, 08028 Barcelona, Spain

ARTICLE INFO

Keywords:
Electro-Fenton
Paracetamol
Photoelectrocatalysis
Sol gel
Solar photoelectro-Fenton
Titanium dioxide

ABSTRACT

An Au-TiO_2 photoanode on carbon cloth has been synthesized by microwave-assisted sol-gel method to treat paracetamol solutions at pH 3.0 by photocatalysis (PC), electro-oxidation (EO), photoelectrocatalysis with UVA light (PEC), solar PEC (SPEC) and hybrid methods with photoelectro-Fenton under UVA (PEC + PEF) and sunlight (SPEC + SPEF) irradiation at constant anodic potential (E_{an}). The photoanode has been characterized by XRD, Raman spectroscopy, HRTEM and SEM-EDS. The counter electrode was a 316L stainless steel plate, which was replaced by an air-diffusion electrode for H_2O_2 generation in hybrid treatments. The most powerful process was SPEC + SPEF, yielding total paracetamol removal in <30 min and 24% mineralization after 180 min, at $E_{an} = +0.82$ V. The paracetamol decay followed a pseudo-first-order kinetics in PEC. A lower rate constant was obtained upon increase of pharmaceutical concentration, showing good linear fit using a Langmuir-Hinshelwood model.

1. Introduction

One of the biggest challenges in the world today is the efficient removal of persistent organic contaminants from water. In particular, pharmaceuticals are routinely detected at concentrations $<10\,\mu g\,L^{-1}$ in sewage treatment plant (STP) effluents [1], further reaching surface water, groundwater and even drinking water. This imposes a variety of negative effects such as endocrine disruption, brain damage, convulsions and carcinogenic diseases [2]. Paracetamol [PCM, *N*-(4-hydroxyphenyl)acetamide] is a top-selling analgesic and antipyretic drug. Concentrations up to $6\,\mu g\,L^{-1}$ have been detected in STP effluents and up to $10\,\mu g\,L^{-1}$ in natural water in USA [3–5]. The complex molecular structure of these residues makes difficult their removal by conventional wastewater treatments [6,7], thus being necessary to develop new materials and technologies.

Advanced oxidation processes (AOPs) have become a suitable choice within this framework, since they allow the generation of hydroxyl radical (•OH) that is a strong oxidant able to non-selectively destroy most organic and organometallic contaminants [8,9]. Paracetamol has been successfully degraded by several AOPs including electrochemical [10,11], ozonation [12], photocatalysis (PC) [13,14], and photoelectrocatalysis (PEC) [15] methods.

PEC is one of the most promising AOPs for the efficient destruction of pharmaceuticals. Among photocatalysts, TiO_2 has received much attention due to its chemical stability, nontoxicity and low cost [13,16]. Nevertheless, its poor photoactivity under visible light irradiation limits its application [17]. Some authors have tried to overcome this drawback via morphological modification (increasing porosity or surface area) or doping with different elements [18,19]. Transition metals such as Co, Fe, Ni, Ag, Au and Pt [20–24] have been used to modify the electronic structure of TiO_2. These metals trap the photogenerated electrons, reducing the electron-hole recombination process [25]. It has also been proven that the synthesis method, yielding particles with different sizes and shapes, plays a key role on the photocatalytic performance [26]. TiO_2 nanopowders can be prepared via various routes like sol gel, chemical vapor deposition, pyrolysis and hydrothermal treat-

* Corresponding authors.
Email addresses: i.sires@ub.edu (I. Sirés); karen.esquivel@uaq.mx (K. Esquivel)
[1] ISE Active Member.

https://doi.org/10.1016/j.elecom.2018.09.009
Received 25 August 2018; Received in revised form 15 September 2018; Accepted 17 September 2018
Available online xxx
1388-2481/

ment [27–30]. The sol-gel technique offers advantages to support metal catalysts, since the active metal and support can be prepared in a single step [31,32]. Recently, novel microwave- and ultrasound-assisted processing methods are also being reported [16,21,33,34].

This work reports the synthesis of a carbon-cloth supported Au-TiO_2 photoanode by microwave-assisted sol-gel method and its application to the removal of paracetamol from aqueous medium by UVA-assisted PEC and solar PEC (SPEC), as well as new hybrid methods with electrochemical AOPs like photoelectro-Fenton (PEF) and solar PEF (SPEF).

2. Materials and methods

2.1. Chemicals

PCM (99.9%) and analytical grade Na_2SO_4, $FeSO_4{\cdot}7H_2O$ and H_2SO_4 were supplied by Fluka and Merck. Solutions were prepared with ultrapure water (Millipore Milli-Q, resistivity >18.2 MΩ cm).

2.2. Synthesis of Au-TiO_2 photocatalyst

A TiO_2 photocatalyst was synthesized as previously reported [17,21]. The titanium precursor (titanium isopropoxide, 99.9%, Sigma-Aldrich) was dissolved in isopropanol (99.9%, Sigma Aldrich) under magnetic stirring for 20 min using nitrogen stream. The hydrolysis process was performed by adding an aqueous gold(III) chloride hydrate (Sigma-Aldrich) solution into the precursor/solvent solution, followed by sodium borohydride addition to ensure chemical reduction to Au, thus obtaining the decorated photocatalyst. The resulting mixture was stirred for 1 h in a dark box and the obtained sol gel was transferred to Teflon vessels to perform the microwave treatment (1800 W, Milestone flexiWAVE), at 210 °C for 30 min. The product was filtered and dried at room temperature for 24 h. After grinding the resulting powder in an agate mortar, it was suspended in an isopropanol/water mixture and electrophoretically deposited on carbon cloth (ElectroChem), at 4 V for 1 min. The final photoanode was calcined at 450 °C for 3 h.

2.3. Structural characterization

The morphological analysis was carried out by high-resolution transmission electron microscopy (HRTEM) using a JEOL 2100 microscope at 200 kV. The sample was dispersed ultrasonically in ethanol and fixed onto a carbon-copper microgrid. Scanning electron microscopy coupled to energy-dispersive X-ray spectroscopy (SEM-EDS) was also employed. The X-ray diffraction (XRD) pattern was obtained with a PANalytical X'Pert PRO MPD Alpha-1 powder diffractometer with Cu $K_{\alpha1}$ radiation (λ = 1.5406 Å). Raman spectra were acquired with a LabRAM HR (Horiba Scientific) with a Nd:YAG laser (λ = 532 nm, output power of 80 mW). Samples were analyzed with a 6 mW power over a 1.5 μm diameter area, using a microscope with a 10× objective. Inductively coupled plasma mass spectrometry (ICP-MS) was carried out in a NexIon 350D equipment to quantify the amount of gold in the catalyst by dissolving the samples in HNO_3/HCl (1:3).

2.4. Photocatalyst performance

The photocatalytic activity of the photoanode was assessed from paracetamol removal using a stirred 78.5 mg L^{-1} solution in 0.050 M Na_2SO_4 at pH 3.0 and 25 °C. In each test, a 100 mL thermostated three-electrode undivided cell, with an Au-TiO_2 (0.1 wt% Au as nominal content) photocatalyst (2 cm^2 algebraic area), Ag/AgCl as reference electrode and a 10 cm^2 316 L stainless steel (SS) plate as counter electrode, was used. All electrolyses were performed with an Amel 2051 potentiostat-galvanostat. A 0.1 L min^{-1} air stream was bubbled through the stirred solution in the dark for 30 min before starting and during the 180 min of each experiment. The system was irradiated with a semicircular UVA lamp containing 18 LEDs (2 W power each, λ = 365 nm). The AOPs applied were: (i) photocatalysis (PC), by irradiating without current supply to electrodes, (ii) electro-oxidation (EO), at anode potential E_{an} = +0.82 V vs Ag/AgCl without irradiation, (iii) PEC and SPEC, at the same potential but under UVA and solar irradiation, respectively, and (iv) two hybrid processes, PEC + PEF and SPEC + SPEF, under the same conditions but adding 0.50 mM $FeSO_4$ and replacing the SS cathode by an air-diffusion electrode to electrogenerate H_2O_2 on site [35]. Solar assays were made in Barcelona, in clear and sunny days of September 2017, with average UV irradiance of 31 W m^{-2}.

2.5. Analytical methods

All samples were filtered with Whatman PTFE filters (0.45 μm) before analysis. Paracetamol concentration decay was followed by high-performance liquid chromatography (HPLC) on a Waters 600 LC fitted with a Spherisorb ODS2 5 μm, 150 mm × 4.6 mm, column at room temperature, and coupled to a photodiode array detector selected at 248 nm. The eluent was a 60:40 (v/v) 10 mM KH_2PO_4/acetonitrile mixture, at 0.8 mL min^{-1}. Paracetamol mineralization was monitored from the removal of total organic carbon (TOC), determined on a Shimadzu VCSN TOC analyzer (50 μL injection volume, 1% accuracy). Experiments were run in duplicate.

3. Results and discussion

3.1. Structural characterization of the Au-TiO_2 photocatalyst

The presence of Au decorating the TiO_2 matrix was corroborated by HRTEM. As can be seen in Fig. 1a, metallic Au nanoparticles can be identified as multiple black dots, whereas TiO_2 formed semi-spherical nanoparticles of 10–12 nm diameter. From FFT analysis, cell parameters of Au-TiO_2 were identified as a = 3.91 Å and c = 8.03 Å. Upon comparison with anatase TiO_2 (a = 3.78 Å, c = 9.52 Å) [19], one can infer cell stress due to Au inclusion. This can also be verified from SEM-EDS and ICP analyses. From EDS analysis of Au-TiO_2 surface (see mapping in Fig. 1b), only 0.04 wt% of Au was detected, whereas ICP showed a higher concentration of 0.08 wt%, which means that Au is not only on the photocatalyst surface but also dissolved inside the crystalline cell.

The X-ray diffractions patterns of several Au-TiO_2 photoanodes are presented in Fig. 2a. Peaks located at 25.3°, 36.9°, 48.0°, 53.9°, 55.1°, corresponding to anatase phase, can be observed in all cases. However, the diffractograms revealed no presence of rutile or Au, probably due to their small concentrations. The calcination process to support the catalyst on carbon cloth did not modify the TiO_2 matrix, as demonstrated by the analogous peaks of the powder. The Raman spectrum of a fresh Au-TiO_2 sample (Fig. 2b) corroborates the presence of anatase phase. The major bands are located at 144, 197, 399, 515, 519 (superimposed with the 515 cm^{-1} band) and 639 cm^{-1} [36]. No rutile phase bands (143, 235, 447, and 612 cm^{-1}) were detected. Although anatase and rutile phases share a common band, note that the one at 144 cm^{-1} is the strongest for anatase and that at 143 cm^{-1} is the weakest one for rutile.

3.2. Activity tests

The performance of the carbon-cloth supported Au-TiO_2 anode was assessed from the treatment of 100 mL of paracetamol solutions with 78.5 mg L^{-1} (50 mg L^{-1} TOC) of the drug containing 0.050 M Na_2SO_4 at pH 3.0 and 25 °C. Fig. 3a evidences that the relative oxidation power of

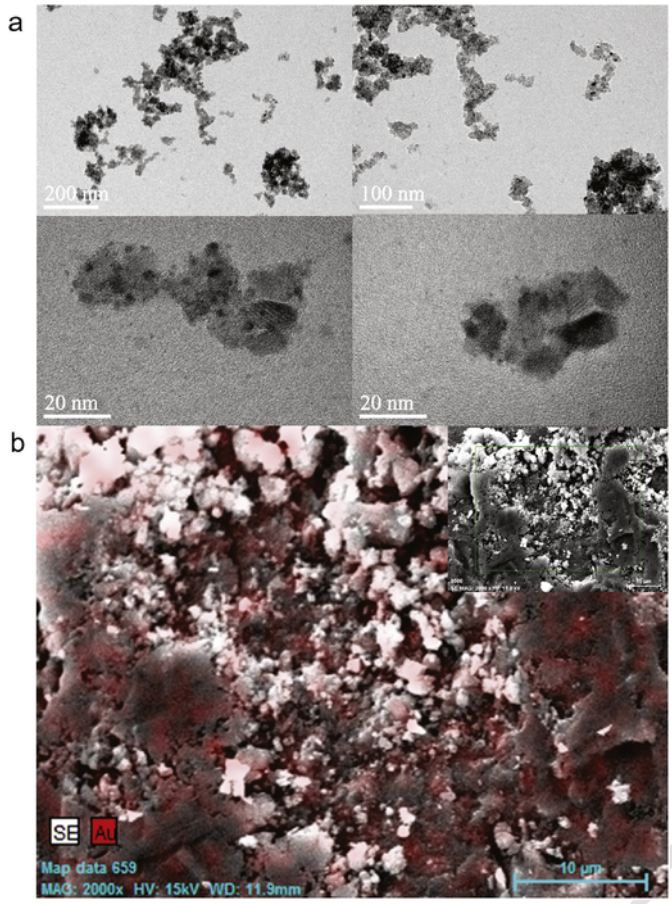

Fig. 1. (a) TEM images and (b) EDS mapping of Au-TiO_2 (0.1 wt% Au) photocatalyst.

AOPs increased as PC ≪ EO < PEC < SPEC ≪ PEC + PEF < SPEC + SPEF, yielding paracetamol removals of 3%, 57%, 62%, 66%, 100% and 100%, respectively. As expected, PC was the less efficient process because the electrons and holes produced from the UVA light absorbed by the photocatalyst via reaction (1) were easily recombined, thus accumulating very low amounts of •OH from reaction (2) [18,19].

$$Au - TiO_2 + h\nu \rightarrow e^-_{CB} + h^+_{VB} \quad (1)$$

$$h^+_{VB} + H_2O \rightarrow {}^{\bullet}OH + H^+ \quad (2)$$

The EO treatment was more powerful due to the greater •OH production at the anode surface from water discharge [6,9]:

$$Au - TiO_2 + H_2O \rightarrow Au - TiO_2({}^{\bullet}OH) + H^+ + e^- \quad (3)$$

The PEC process yielded a final paracetamol degradation quite similar to the sum of PC (3%) and EO (57%). This suggests that PEC pre-eminently involves the oxidation with •OH independently formed from reactions (2) and (3). The better removal in SPEC can be related to greater generation of holes and •OH upon use of powerful radiation, along with a smaller electron-hole recombination because the dopant Au trapped some of the photoelectrons. The Au-TiO_2 photoanode then results efficient under sunlight illumination.

The hybrid methods led to much faster degradation since in PEF, a great quantity of •OH is formed in the bulk from Fenton's reaction (4), as well as from photolytic reaction (5) [6,8]. The combined action of these radicals with those originated from reactions (2) and (3) explains the fast and overall paracetamol abatement after 45 min of PEC + PEF treatment. This time was shortened to 25 min in SPEC + SPEF because of the acceleration of reactions (1), (2) and (5) [6].

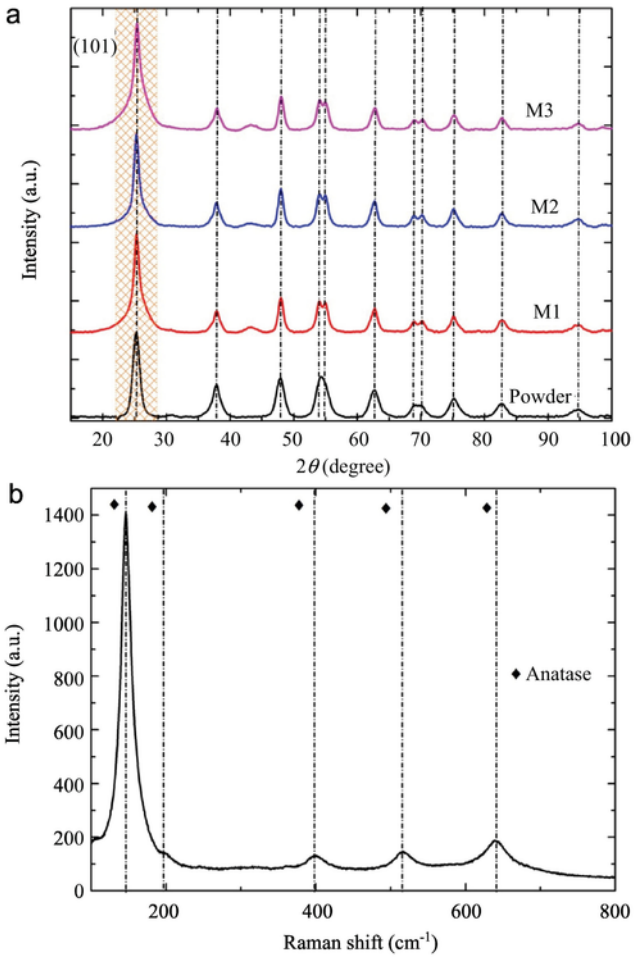

Fig. 2. (a) X-ray diffraction patterns of: (i) M1, fresh photoanode, (ii) M2, photoanode used in PEC, (iii) M3, damaged photoanode, and (iv) Au-TiO_2 (0.1 wt% Au) powder. (b) Raman spectrum of the same powder.

$$H_2O_2 + Fe^{2+} \rightarrow Fe^{3+} + {}^{\bullet}OH + OH^- \quad (4)$$

$$Fe(OH)^{2+} + h\nu \rightarrow Fe^{2+} + {}^{\bullet}OH \quad (5)$$

The solution TOC was only abated in PEC + PEF and SPEC + SPEF, finally achieving about 20% and 24% mineralization, respectively, verifying the higher power of the latter.

To gain better insight into PEC process, tests were performed with initial paracetamol concentration ($[PCM]_0$) between 15.7 and 78.6 mg L^{-1}. Similar profiles for the normalized concentration removals, slightly faster at smaller content, were obtained. A degradation of 65% and 60% was found when the concentrations increased from 15.7 to 78.6 mg L^{-1}. No mineralization was found during these trials.

The above concentration decays fitted well with pseudo-first-order kinetic model, and Fig. 3b highlights a gradual drop of the corresponding rate constant (k_1) from 9.34 × 10^{-3} to 5.48 × 10^{-3} min^{-1} when $[PCM]_0$ rose from 15.7 to 78.6 mg L^{-1}. This tendency means that k_1 is not a true rate constant, since it should be $[PCM]_0$-independent. The decay of k_1 at increasing drug concentration can be associated with

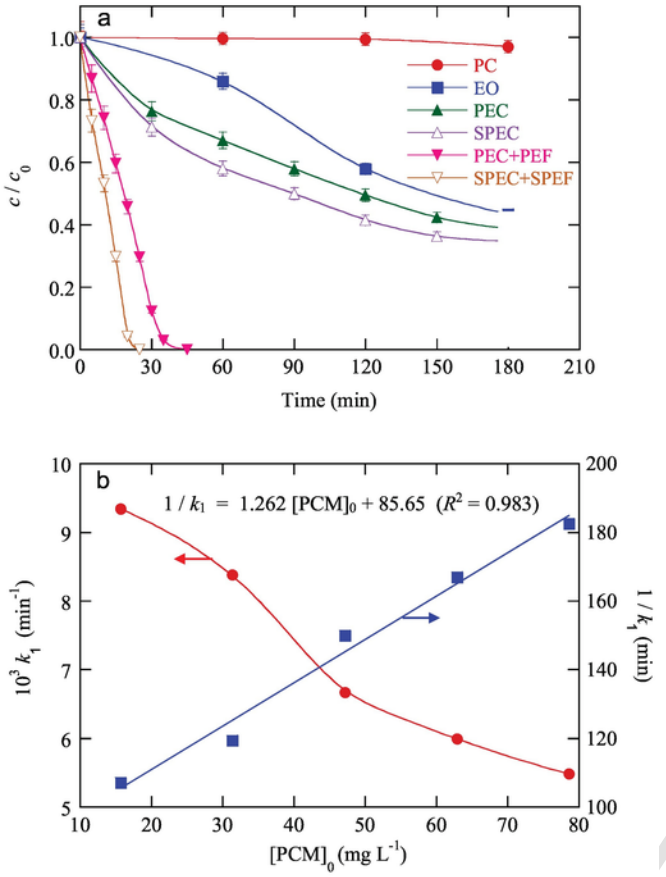

Fig. 3. (a) Normalized paracetamol decay vs. reaction time for the treatment of 100 mL of 78.6 mg L^{-1} drug at pH 3.0 by AOPs. (b) Change of rate constant and its reciprocal with paracetamol concentration upon PEC treatments.

two factors: (i) larger adsorption of paracetamol molecules onto Au-TiO_2 active sites, and (ii) larger absorption of photons by paracetamol. This leads to a smaller photon absorption by Au-TiO_2, causing a lower generation of electron-hole pairs that ends in a lower amount of •OH from reaction (2). The Langmuir-Hinshelwood model was applied to justify the change of k_1 with $[PCM]_0$, verifying the following relationship [37]:

$$\frac{1}{k_1} = \frac{1}{k_c K_{PCM}} + \frac{1}{k_c}[PCM]_0 \quad (6)$$

where k_c is the rate constant at the catalyst surface and K_{PCM} is the Langmuir-Hinshelwood adsorption equilibrium constant. Fig. 3c shows the good linear $1/k_1$ vs. $[PCM]_0$ trend, with $R^2 = 0.983$, yielding $k_c = 0.792$ mg L^{-1} min^{-1} and $K_{PCM} = 0.0073$ L mg^{-1}. These results inform about a fast reaction of paracetamol with •OH, along with poor adsorption, at the Au-TiO_2 surface.

4. Conclusions

An Au-TiO_2 photoanode supported on carbon cloth was successfully synthesized by microwave-assisted sol gel. The main crystalline phase was anatase and tensions on the TiO_2 structure were detected. PEC process yielded 62% paracetamol degradation, being enhanced to 66% under sunlight radiation in SPEC. This demonstrated the ability to absorb visible light thanks to Au doping. A larger removal was found using hybrid PEC + PEF and SPEC + SPEF processes, due to the additional powerful action of •OH formed under Fenton conditions. The most efficient treatment was SPEC + SPEF, allowing 100% degradation at 25 min and 24% mineralization after 180 min. In PEC, paracetamol decays obeyed a pseudo-first-order kinetics, and Langmuir-Hinshelwood model showed a fast surface reaction with poor adsorption of paracetamol molecules.

Acknowledgements

The authors acknowledge financial support from project CTQ2016-78616-R (AEI/FEDER, EU), and the PhD grant awarded to R. Hernández by CONACYT (Mexico) to do this work.

References

[1] T.A. Ternes, M. Meisenheimer, D. McDowell, F. Sacher, H.-J. Brauch, B. Haist-Gulde, G. Preuss, U. Wilme, N. Zulei-Seibert, Removal of pharmaceuticals during drinking water treatment, Environ. Sci. Technol. 36 (2002) 3855–3863, https://doi.org/10.1021/es015757k.

[2] J.O. Tijani, O.O. Fatoba, L.F. Petrik, A review of pharmaceuticals and endocrine-disrupting compounds: sources, effects, removal, and detections, Water Air Soil Pollut. 224 (2013) 1770–1799, https://doi.org/10.1007/s11270-013-1770-3.

[3] D.W. Kolpin, E.T. Furlong, M.T. Meyer, E.M. Thurman, S.D. Zaugg, L.B. Barber, H.T. Buxton, Pharmaceuticals, hormones, and other organic wastewater contaminants in U.S. Streams, 1999–2000: a national reconnaissance, Environ. Sci. Technol. 36 (2002) 1202–1211, https://doi.org/10.1021/es011055j.

[4] M. Petrovic, J. Radjenovic, C. Postigo, M. Kuster, M. Farre, M.L. de Alda, D. Barceló, Emerging contaminants in waste waters: sources and occurrence, in: D. Barceló, M. Petrovic (Eds.), Emerging Contaminants From Industrial and Municipal Waste, Springer-Verlag, Berlin, Heidelberg, 2008, pp. 1–35, https://doi.org/10.1007/698_5_106.

[5] L. Yang, L.E. Yu, M.B. Ray, Degradation of paracetamol in aqueous solutions by TiO_2 photocatalysis, Water Res. 42 (2008) 3480–3488, https://doi.org/10.1016/j.watres.2008.04.023.

[6] I. Sirés, E. Brillas, Remediation of water pollution caused by pharmaceutical residues based on electrochemical separation and degradation technologies: a review, Environ. Int. 40 (2012) 212–229, https://doi.org/10.1016/j.envint.2011.07.012.

[7] R. Daghrir, P. Drogui, D. Robert, Modified TiO_2 for environmental photocatalytic applications: a review, Ind. Eng. Chem. Res. 52 (2013) 3581–3599, https://doi.org/10.1021/ie303468t.

[8] E. Brillas, I. Sirés, M.A. Oturan, Electro-Fenton process and related electrochemical technologies based on Fenton's reaction chemistry, Chem. Rev. 109 (2009) 6570–6631, https://doi.org/10.1021/cr900136g.

[9] I. Sirés, E. Brillas, M.A. Oturan, M.A. Rodrigo, M. Panizza, Electrochemical advanced oxidation processes: today and tomorrow. A review, Environ. Sci. Pollut. Res. 21 (2014) 8336–8367, https://doi.org/10.1007/s11356-014-2783-1.

[10] E. Brillas, I. Sirés, C. Arias, P.L. Cabot, F. Centellas, R.M. Rodríguez, J.A. Garrido, Mineralization of paracetamol in aqueous medium by anodic oxidation with a boron-doped diamond electrode, Chemosphere 58 (2005) 399–406, https://doi.org/10.1016/j.chemosphere.2004.09.028.

[11] I. Sirés, J.A. Garrido, R.M. Rodríguez, P.L. Cabot, F. Centellas, C. Arias, E. Brillas, Electrochemical degradation of paracetamol from water by catalytic action of Fe^{2+}, Cu^{2+}, and UVA light on electrogenerated hydrogen peroxide, J. Electrochem. Soc. 153 (2006) D1–D9, https://doi.org/10.1149/1.2130568.

[12] A. Ziylan-Yavaş, N.H. Ince, Catalytic ozonation of paracetamol using commercial and Pt-supported nanocomposites of Al_2O_3: the impact of ultrasound, Ultrason. Sonochem. 40 (2018) 175–182, https://doi.org/10.1016/j.ultsonch.2017.02.017.

[13] L. Yang, L.E. Yu, M.B. Ray, Photocatalytic oxidation of paracetamol: dominant reactants, intermediates, and reaction mechanisms, Environ. Sci. Technol. 43 (2009) 460–465, https://doi.org/10.1021/es8020099.

[14] E. Moctezuma, E. Leyva, C.A. Aguilar, R.A. Luna, C. Montalvo, Photocatalytic degradation of paracetamol: intermediates and total reaction mechanism, J. Hazard. Mater. 243 (2012) 130–138, https://doi.org/10.1016/j.jhazmat.2012.10.010.

[15] H.C. Arredondo-Valdez, G. García-Jiménez, S. Gutiérrez-Granados, C. Ponce de León, Degradation of paracetamol by advance oxidation processes using modified reticulated vitreous carbon electrodes with TiO_2 and $CuO/TiO_2/Al_2O_3$, Chemosphere 89 (2012) 1195–1201, https://doi.org/10.1016/j.chemosphere.2012.07.020.

[16] D.P. Macwan, P.N. Dave, S. Chaturvedi, A review on nano-TiO_2 sol–gel type syntheses and its applications, J. Mater. Sci. 46 (2011) 3669–3686, https://doi.org/10.1007/s10853-011-5378-y.

[17] R. Hernández, S.M. Durón-Torres, K. Esquivel, C. Guzmán, Microwave assisted sol-gel synthesis and characterization of M–TiO_2 (M = Pt, Au) photocatalysts, In: Characterization of Metals and Alloys, Springer, Switzerland, 2017, pp. 183–189, https://doi.org/10.1007/978-3-319-31694-9_15.

[18] J. Zhou, X.S. Zhao, Visible-light-responsive titanium dioxide photocatalysts, in: M. Anpo, P.V. Kamat (Eds.), Environmentally Benign Photocatalysts, Springer, New York, 2010, pp. 235–251, https://doi.org/10.1007/978-0-387-48444-0_10.

[19] M. Pelaez, N.T. Nolan, S.C. Pillai, M.K. Seery, P. Falaras, A.G. Kontos, P.S.M. Dunlop, J.W.J. Hamilton, J.A. Byrne, K. O'Shea, M.H. Entezari, D.D. Dionysiou, A review on the visible light active titanium dioxide photocatalysts for environmental

applications, Appl. Catal. B Environ. 125 (2012) 331–349, https://doi.org/10.1016/j.apcatb.2012.05.036.
[20] M.D. Hernández-Alonso, F. Fresno, S. Suárez, J.M. Coronado, Development of alternative photocatalysts to TiO_2: challenges and opportunities, Energy Environ. Sci. 2 (2009) 1231–1257, https://doi.org/10.1039/B907933E.
[21] K. Esquivel, R. Nava, A. Zamudio-Méndez, M.V. González, O.E. Jaime-Acuña, L. Escobar-Alarcón, J.M. Peralta-Hernández, B. Pawelec, J.L.G. Fierro, Microwave-assisted synthesis of (S)Fe/TiO_2 systems: effects of synthesis conditions and dopant concentration on photoactivity, Appl. Catal. B Environ. 140–141 (2013) 213–224, https://doi.org/10.1016/j.apcatb.2013.03.047.
[22] W. Khan Alamgir, S. Ahmad, M. Mehedi Hassan, A.H. Naqvi, Structural phase analysis, band gap tuning and fluorescence properties of Co doped TiO_2 nanoparticles, Opt. Mater. 38 (2014) 278–285, https://doi.org/10.1016/j.optmat.2014.10.054.
[23] A. Cybula, G. Nowaczyk, M. Jarek, A. Zaleska, A. Cybula, G. Nowaczyk, M. Jarek, A. Zaleska, Preparation and characterization of Au/Pd modified-TiO_2 photocatalysts for phenol and toluene degradation under visible light. The effect of calcination temperature, J. Nanomater. 2014 (2014)e918607https://doi.org/10.1155/2014/918607.
[24] M.P. Blanco-Vega, J.L. Guzmán-Mar, M. Villanueva-Rodríguez, L. Maya-Treviño, L.L. Garza-Tovar, A. Hernández-Ramírez, L. Hinojosa-Reyes, Photocatalytic elimination of bisphenol A under visible light using Ni-doped TiO_2 synthesized by microwave assisted sol-gel method, Mater. Sci. Semicond. Process. 71 (2017) 275–282, https://doi.org/10.1016/j.mssp.2017.08.013.
[25] J. Zhang, Y. Cong, M. Anpo, Chemical methods for the preparation of multifunctional photocatalysts, in: M. Anpo, P.V. Kamat (Eds.), Environmentally Benign Photocatalysts, Springer, New York, 2010, pp. 7–33, https://doi.org/10.1007/978-0-387-48444-0_2.
[26] S.G. Kumar, L.G. Devi, Review on modified TiO_2 photocatalysis under UV/visible light: selected results and related mechanisms on interfacial charge carrier transfer dynamics, J. Phys. Chem. A 115 (2011) 13211–13241, https://doi.org/10.1021/jp204364a.
[27] M. Reinke, E. Ponomarev, Y. Kuzminykh, P. Hoffmann, Combinatorial characterization of TiO_2 chemical vapor deposition utilizing titanium isopropoxide, ACS Comb. Sci. 17 (2015) 413–420, https://doi.org/10.1021/acscombsci.5b00040.
[28] C.G. Aba-Guevara, I.E. Medina-Ramírez, A. Hernández-Ramírez, J. Jáuregui-Rincón, J.A. Lozano-Álvarez, J.L. Rodríguez-López, Comparison of two synthesis methods on the preparation of Fe, N-Co-doped TiO_2 materials for degradation of pharmaceutical compounds under visible light, Ceram. Int. 43 (2017) 5068–5079, https://doi.org/10.1016/j.ceramint.2017.01.018.
[29] S. Alwin, X.S. Shajan, K. Karuppasamy, K.G.K. Warrier, Microwave assisted synthesis of high surface area TiO_2 aerogels: competent photoanode material for quasi-solid dye-sensitized solar cells, Mater. Chem. Phys. 196 (2017) 37–44, https://doi.org/10.1016/j.matchemphys.2017.04.045.
[30] M. Košević, S. Stopic, A. Bulan, J. Kintrup, R. Weber, J. Stevanović, V. Panić, B. Friedrich, A continuous process for the ultrasonic spray pyrolysis synthesis of RuO_2/TiO_2 particles and their application as a coating of activated titanium anode, Adv. Powder Technol. 28 (2017) 43–49, https://doi.org/10.1016/j.apt.2016.07.015.
[31] E. Sánchez, T. López, R. Gómez, Bokhimi, A. Morales, O. Novaro, Synthesis and characterization of sol–gel Pt/TiO_2 catalyst, J. Solid State Chem. 122 (1996) 309–314, https://doi.org/10.1006/jssc.1996.0118.
[32] M. Jasiorski, B. Borak, A. Łukowiak, A. Baszczuk, Active sol-gel materials, in: P. Innocenzi, Y.L. Zub, V.G. Kessler (Eds.), Sol-gel Methods for Materials Processing, Springer, Netherlands, 2008, pp. 125–137, https://doi.org/10.1007/978-1-4020-8514-7_8.
[33] M. Fernández-García, A. Martínez-Arias, J.C. Conesa, Visible light-responsive titanium oxide photocatalysts: preparations based on chemical methods, In: Environmental Benign Photocatalysis, Springer, New York, 2010, pp. 277–299, https://doi.org/10.1007/978-0-387-48444-0_12.
[34] C. Han, J. Andersen, S.C. Pillai, R. Fagan, P. Falaras, J.A. Byrne, P.S.M. Dunlop, H. Choi, W. Jiang, K. O'Shea, D.D. Dionysiou, Green nanotechnology: development of nanomaterials for environmental and energy applications, In: Sustainable Nanotechnology and the Environment Advances and Achievements, American Chemical Society, 2013, pp. 201–229, https://doi.org/10.1021/bk-2013-1124.ch012.
[35] A. Galia, S. Lanzalaco, M.A. Sabatino, C. Dispenza, O. Scialdone, I. Sirés, Crosslinking of poly(vinylpyrrolidone) activated by electrogenerated hydroxyl radicals: a first step towards a simple and cheap synthetic route of nanogel vectors, Electrochem. Commun. 62 (2016) 64–68, https://doi.org/10.1016/j.elecom.2015.12.005.
[36] J. Zhang, Q. Xu, Z. Feng, C. Li, UV Raman spectroscopic studies on titania: phase transformation and significance of surface phase in photocatalysis, in: M. Anpo, P.V. Kamat (Eds.), Environmentally Benign Photocatalysts, Springer, New York, 2010, pp. 153–184, https://doi.org/10.1007/978-0-387-48444-0_6.
[37] K. Vasanth Kumar, K. Porkodi, F. Rocha, Langmuir–Hinshelwood kinetics – a theoretical study, Catal. Commun. 9 (2008) 82–84, https://doi.org/10.1016/j.catcom.2007.05.019.